



Single phase materials based on Co-doped SrTiO₃ for mixed ionic-electronic conductors applications

A. Murashkina^a, V. Maragou^b, D. Medvedev^a, V. Sergeeva^a, A. Demin^{a,*}, P. Tsiakaras^{b,**}

^a Institute of High Temperature Electrochemistry, Laboratory of Solid Oxide Fuel Cells, 22 S. Kovalevskoy, 620990 Yekaterinburg, Russia

^b Department of Mechanical Engineering, School of Engineering, University of Thessaly, Pedion Areos, 383 34 Volos, Greece

ARTICLE INFO

Article history:

Received 7 October 2011

Received in revised form 12 February 2012

Accepted 17 February 2012

Available online 17 March 2012

Keywords:

Cobalt oxide

Strontium titanates

Mixed ionic–electronic conductors

Oxygen permeability

ABSTRACT

In the present work the effect of cobalt oxide addition on the structural and electrical properties of strontium titanate is examined. The SrTi_{1-x}Co_xO_{3-δ} (0 ≤ x ≤ 0.4) samples were synthesized according to solid state reaction method at 1150 °C and sintered at 1400 °C. The samples are single phase and crystallize in the cubic perovskite-type structure. With the increase of cobalt content the lattice parameter of the cubic cell is reduced, due to dimensional factor. The most dense sample is obtained for x = 0.2. The electrical conductivity is examined by 4-probe dc-technique in the range of 600–1000 °C in air atmosphere, as well as in a wide range of oxygen partial pressures (pO₂ = 1 × 10⁻¹⁹–0.21 atm) at 900 °C. The conductivity dependence on pO₂ can be explained by using the formalism of quasi-chemical reactions. The single-phase materials exhibit poor stability in reducing atmosphere (hydrogen) and good stability in salt-forming (carbon dioxide) components. In the oxidative region, the samples are characterized by mixed ionic-type conduction, and therefore can be used as membranes in high-temperature electrochemical devices; as for example, for oxygen production. The oxygen permeability and the thermal expansion measurements confirm that the specific materials can be used in electrochemical devices.

© 2012 Elsevier B.V. All rights reserved.

1. Introduction

Specific oxides that are characterized by mixed ionic–electronic conductivity (MIEC) are promising materials for membranes used for the electrochemical production of oxygen from gas mixtures. Among the investigated oxides, perovskite-like materials based on titanates of alkaline earth elements have attracted considerable attention, due to their satisfying stability in severe environment [1]. Titanates of alkaline earth elements that present mixed ionic–electronic conductivity can be used in electrochemical devices for hydrogen or oxygen production [2]. However, this kind of applications requires also high values of ambipolar conductivity and stability in severe environment (high gradient of pO₂, high temperatures and thermocycling). Therefore, the development of novel materials that will maintain optimal properties during long term operation is requisite. The properties of oxide systems can be varied in a wide range by doping with an acceptor or donor agent in a sublattice of rare earth elements or/and in the sublattice of titanium [3–8]. For pure and acceptor doped SrTiO₃, there is a transition from n- to p-type regions with increasing the oxygen partial pressure (pO₂) [5]. The onset of the p-type conduction at the

conductivity minimum depends on the type and the amount of the acceptor impurity added to SrTiO₃ [5].

As far as it concerns SrFe_{0.2-x}Ti_{0.8}Co_xO_{3-δ} materials, a significant increase of the grain size was observed with the increase of cobalt's concentration in the samples [9]. Additionally, the lattice of these samples was compressed due to the formation of oxygen vacancies and the electrical conductivity increased. It was found that in the case of SrFe_{0.2-x}Ti_{0.8}Co_xO_{3-δ} (x = 0.05–0.2) samples, the iron rich and completely cobalt substituted samples exhibit good change in electrical conductivity between 21% O₂ and 10 ppm O₂ in argon [9]. In the case of SrCo_{1-x}Ti_xO_{3-δ} system, in the work of Kharton et al. it was found that the oxygen permeability increases with the increase of titanium concentration [10]. The present work aims at the investigation of the structural, electrical and thermomechanical properties of Co-doped SrTiO₃ in a wide range of operation conditions, in order to determine the suitability of the prepared materials for applications in electrochemical devices.

2. Experimental

The SrTi_{1-x}Co_xO_{3-δ} (x = 0–0.4, Δx = 0.05) samples were synthesized according to the standard ceramic technology. In order to eliminate hydration effects, the powders were heated beforehand in air (SrCO₃, Co₃O₄ at 200 °C, TiO₂ at 800 °C). The stoichiometric mixture was synthesized at 1150 °C in air for 5 h (heating/cooling

* Corresponding author. Tel.: +7 343 3745431.

** Corresponding author. Tel.: +30 24210 74065; fax: +30 24210 74050.

E-mail addresses: ademini@ihte.uran.ru (A. Demin), tsiak@uth.gr (P. Tsiakaras).

rate of $300\text{ }^{\circ}\text{C h}^{-1}$). After preliminary calcinations, these powders were ground in an agate mortar in acetone for 30 min and then a 4% solution of SKN26-M (Omsky Caoutchouc Company, Russia) in a mixture of acetone and gasoline at a ratio of 3:2 was added to the powder. The resulting mixture was poured onto a fluoroplastic substrate. The dried film was rolled to 1 mm thick plates using a roller machine and then $20\text{ mm} \times 5\text{ mm} \times 1\text{ mm}$ bars were cut from the plates. The bars were heated to $600\text{ }^{\circ}\text{C}$ in air for 5 h with heating/cooling rate of $1\text{ }^{\circ}\text{C min}^{-1}$. Then the samples were heated to $1400\text{ }^{\circ}\text{C}$ at $5\text{ }^{\circ}\text{C min}^{-1}$ for 5 h in air. The density of the sintered ceramic samples determined by the hydrostatic weighting method in kerosene was no less than 96% of the density calculated from the XRD data.

The XRD analyses were carried out by using a DMAX-2500, Rigaku Co. Ltd., Japan device in $\text{CuK}\alpha$ radiation in $15^{\circ} \leq 2\theta \leq 85^{\circ}$. The unit cell parameters were defined using XRD data. The morphology and the structure of the ceramic membranes' surface were determined with the aid of scanning electron microscopy (JSM-5500 LV JEOL microscope). The conductivity of the as-prepared samples was investigated by using the standard four probe dc-method, in a wide range of temperatures, as well as in a wide range of oxygen partial pressures (1×10^{-19} – 0.21 atm) at $900\text{ }^{\circ}\text{C}$. The experimental details of the oxygen permeability measurements were presented in a previous work [11]. Finally, the thermal expansion was measured in air during heating from room temperature to $900\text{ }^{\circ}\text{C}$ using a quartz dilatometer, with a heating/cooling rate of $200\text{ }^{\circ}\text{C h}^{-1}$. The bar-shaped ceramic samples were prepared in the same way as those for the electrical conductivity measurements.

3. Results and discussion

In Fig. 1 typical XRD patterns of the $\text{SrTi}_{1-x}\text{Co}_x\text{O}_{3-\delta}$ samples are presented (SrTiO_3 – JCPDS No. 73-0661). Solid solutions with perovskite cubic structure (space group $Pm3m$) based on strontium titanate are formed. The obtained results are consistent with already published data. More precisely, in the case of SrTiO_3 the lattice parameter of the unit cell has been reported to be equal to 3.905 \AA [12], whereas in the case of $\text{SrTi}_{0.8}\text{Co}_{0.2}\text{O}_{3-\delta}$ 3.895 \AA [9], which are in good agreement with the data of the present work. The volume of a cubic unit cell decreases with the increase of the cobalt content. The observed behavior can be attributed to the fact that the ionic radius of Co^{4+} ($r = 0.530\text{ \AA}$) is smaller in comparison to the radius of Ti^{4+} ($r = 0.605\text{ \AA}$). In the work of Souza et al. where the system $\text{Sr}_{1-x}\text{Co}_x\text{TiO}_3$ was investigated, it was found that the lattice parameters decrease when the amount of cobalt increases, due to its smaller ionic radius [13]. However, the slow decrease of the unit

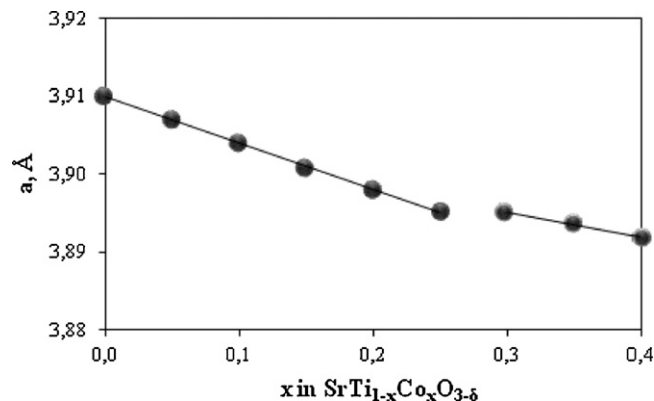


Fig. 2. Lattice parameters as a function of Co-content in $\text{SrTi}_{1-x}\text{Co}_x\text{O}_{3-\delta}$.

cubic cell along with the increase of x is probably connected with the mixed valence state of cobalt Co^{+3} – Co^{+4} [12]. Therefore, the average effective radius of cobalt increases (Co^{3+} , $r = 0.610\text{ \AA}$). As shown in Fig. 2, the lattice parameters' dependence as a function of Co-content in $\text{SrTi}_{1-x}\text{Co}_x\text{O}_{3-\delta}$ does not obey Vegard's principle. The sharp curve is observed in the concentration range of $x = 0.25$ – 0.30 . The non-linear dependence may derive from the existence of an isostructural phase of strontium cobaltite, which has characteristic peaks at the same angles as the phase of strontium titanate, and therefore they are not detectable by XRD. The formation of isostructural phases were also observed by other authors [14,15]. In the work of Kharton et al. it was found that in the oxide system $\text{SrCoO}_{3-\delta}$ – SrTiO_3 , in air and at temperatures below $1277\text{ }^{\circ}\text{C}$, two concentration ranges exist in which isostructural solid solutions with perovskite-like cubic crystal lattice form. The concentration range, in which both isostructural phases coexisted in $\text{SrCo}_{1-x}\text{Ti}_x\text{O}_{3-\delta}$, corresponded to $0.3 \leq x \leq 0.7$ [14]. According to the results of Pascanut et al. the homogeneity of the solution on the basis of cobaltite extends to 50 mol.% [15].

In Fig. 3, the SEM images of the as-sintered $\text{SrTi}_{1-x}\text{Co}_x\text{O}_{3-\delta}$ ($x = 0.0, 0.1, 0.2$ and 0.3) samples are presented. It can be observed that fine micro-structure with good connected grains and small amount of pores is observed for $\text{SrTi}_{1-x}\text{Co}_x\text{O}_{3-\delta}$ sintered at $1400\text{ }^{\circ}\text{C}$. At the same time, the Co addition results in a slight increase of relative densities of the ceramics with non-porous structure. In the case of SrTiO_3 and $\text{SrTi}_{0.9}\text{Co}_{0.1}\text{O}_{3-\delta}$, several fractions are distinguished: the fraction of grains with size less than $1\text{ }\mu\text{m}$ and the fraction of grains with an average size of approximately $6\text{ }\mu\text{m}$. If the sintering process for these samples was incomplete, the presence of smaller and large grains, as well as porosity may have been observed. Moreover, pores with diameter of $10\text{ }\mu\text{m}$ exist on the surface of SrTiO_3 and $\text{SrTi}_{0.9}\text{Co}_{0.1}\text{O}_{3-\delta}$ samples. The $\text{SrTi}_{0.8}\text{Co}_{0.2}\text{O}_{3-\delta}$ sample's surface is nonporous and consists of grains with size of ~ 5 – $7\text{ }\mu\text{m}$. Finally, in the case of $\text{SrTi}_{0.7}\text{Co}_{0.3}\text{O}_{3-\delta}$ the grain size corresponds to 3 – $8\text{ }\mu\text{m}$ and practically has no pores.

In Fig. 4 the temperature dependence of the electrical conductivity in air of the $\text{SrTi}_{1-x}\text{Co}_x\text{O}_{3-\delta}$ system is presented in Arrhenius coordinates. These materials have a semiconducting type of conductivity in the temperature range of 600 – $1000\text{ }^{\circ}\text{C}$. The conductivity increases with the increase of cobalt concentration. The maximum value for single-phase samples ($x = 0.25$) is 303.1 mS cm^{-1} at $1000\text{ }^{\circ}\text{C}$.

Fig. 5 shows the dependence of the electrical conductivity on the oxygen partial pressure at $900\text{ }^{\circ}\text{C}$. The SrTiO_3 sample presents p-type of conductivity at oxidizing atmosphere and n-type of conductivity at reducing atmosphere. As seen in the graph, the increase of cobalt concentration leads to the increase of the electrical conductivity throughout the range of the oxygen partial pressure, which is maximized in the case of $x = 0.25$. This change of

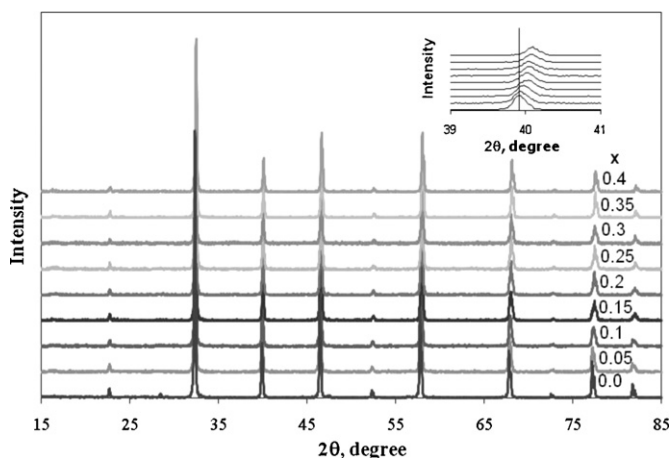


Fig. 1. Room temperature XRD data for the samples of $\text{SrTi}_{1-x}\text{Co}_x\text{O}_{3-\delta}$.

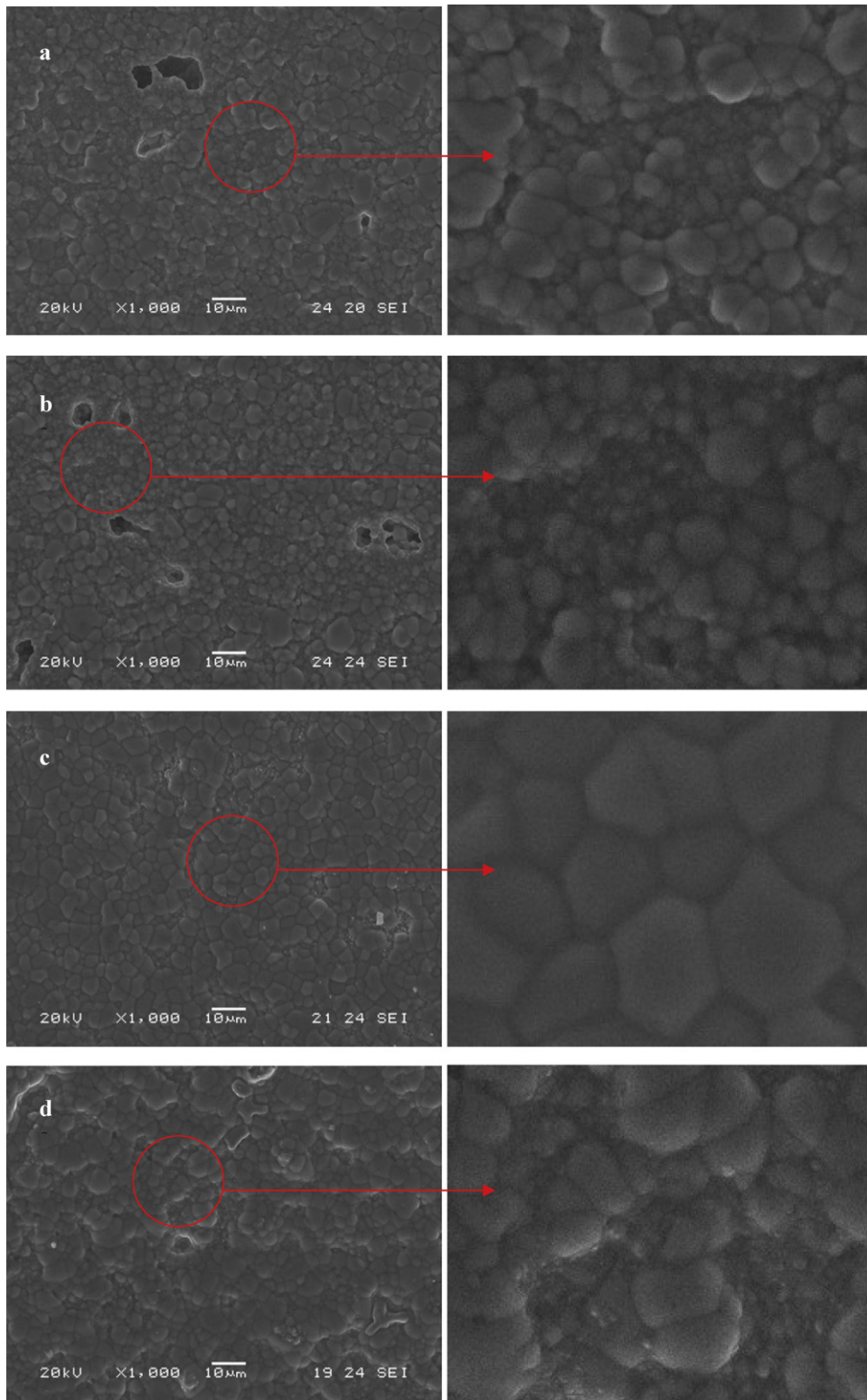
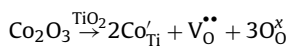


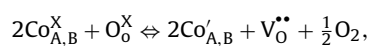
Fig. 3. SEM micrographs of the surfaces of the as sintered SrTi_{1-x}Co_xO_{3-δ} samples; a – x = 0, b – x = 0.1, c – x = 0.2, d – x = 0.3.

conductivity can be attributed to the increase of the oxygen-ionic conductivity which results from the formation of Koch–Wagner defects:



At this point it is worth mentioning that the valence state of cobalt element in Co-modified ABO₃ perovskite materials, usually,

is mixed and determined by the nature of A and B elements, the type of other dopants (acceptor, donor) and the conditions of the atmosphere (*p*O₂, T), according to the following equilibrium reactions:



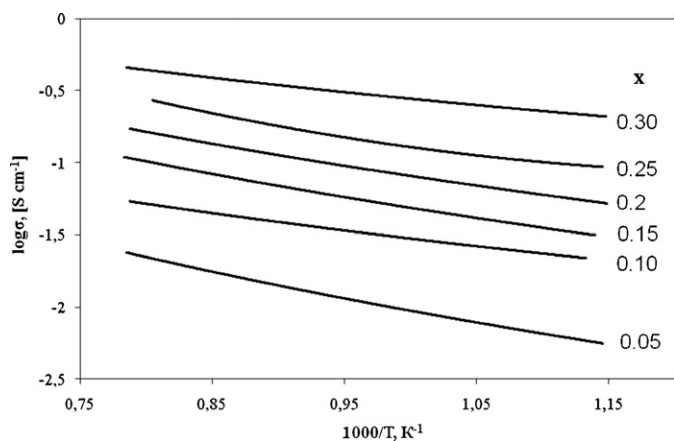
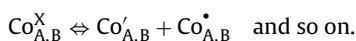


Fig. 4. Temperature dependence of total conductivity of $\text{SrTi}_{1-x}\text{Co}_x\text{O}_{3-\delta}$ samples in air.



In the part concerning Fig. 2 the fact that the lattice parameters are decreased slowly with the increase of x , can be connected with the mixed state of Co-ions. We noted that Co ions simultaneously exist as Co^{3+} and as Co^{4+} . Concerning Fig. 5, the increase of conductivity at the same time, is connected with the oxygen vacancy formation by the partial substitution of Ce^{4+} ions by Co^{3+} cobalt ions.

With increasing Co-content in strontium titanate, the part of p-conductivity was found to decrease. For the samples with $x=0, 0.05, 0.1, 0.15, 0.2, 0.25$ the transfer number of hole conductivity was estimated from Fig. 5 at $p\text{O}_2 = 0.21$ atm and was found to be equal to 0.85, 0.58, 0.47, 0.43, 0.39, 0.37, respectively. At the same time, the value of the hole conductivity at $\log(p\text{O}_2/\text{atm}) = -0.6$ increases from 0.7 mS cm^{-1} at $x=0$ to 80 mS cm^{-1} at $x=0.25$. In the interval of intermediate $p\text{O}_2$, the conductivity of Co-doped samples is constant and corresponds to the oxygen-ionic conductivity. The decrease of $p\text{O}_2$ to 1×10^{-20} atm results in the strong decrease of the Co-doped samples' conductivity. In addition, the breaking point of the dependence $\log \sigma \div \log p\text{O}_2$ shifts to higher values while increasing Co-content in strontium titanate, from $p\text{O}_2 = 1 \times 10^{-14.5}$ atm at $x=0.05$ to $p\text{O}_2 = 1 \times 10^{-12}$ atm at $x=0.25$. The given dependence can be connected with the process of Co reduction in the $\text{SrTi}_{1-x}\text{Co}_x\text{O}_{3-\delta}$ samples. The conductivities of the Co-doped samples at $p\text{O}_2 = 1 \times 10^{-19} - 1 \times 10^{-18}$ atm is equal for all quantities of dopant.

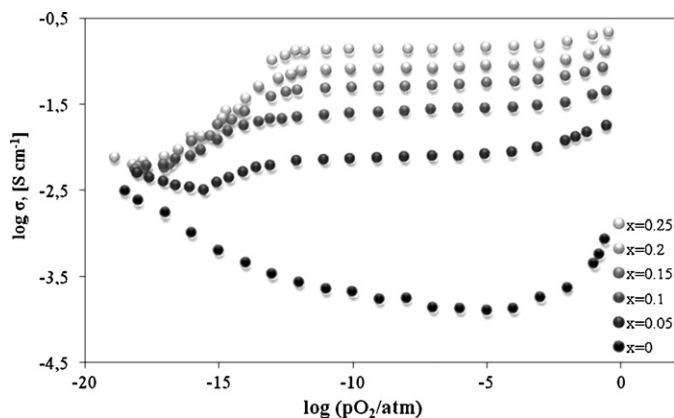


Fig. 5. Oxygen partial pressure dependence of the electrical conductivity of $\text{SrTi}_{1-x}\text{Co}_x\text{O}_{3-\delta}$ samples at 900°C .

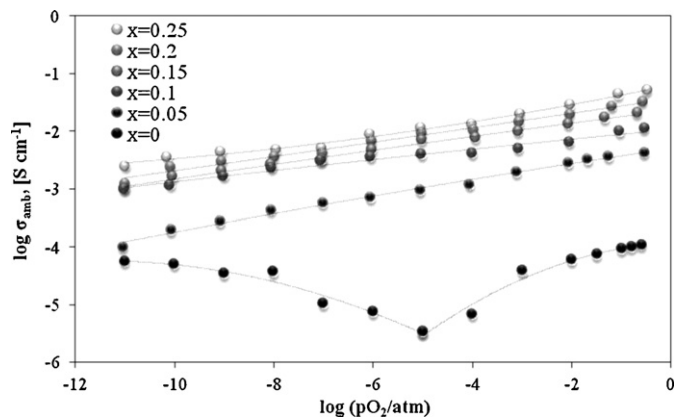


Fig. 6. Oxygen partial pressure dependence of ambipolar conductivity of $\text{SrTi}_{1-x}\text{Co}_x\text{O}_{3-\delta}$ samples at 900°C .

By using the data of Fig. 5 the values of ambipolar conductivity were calculated. The dependences of ambipolar conductivity of $\text{SrTi}_{1-x}\text{Co}_x\text{O}_{3-\delta}$ samples on the partial pressure of oxygen in the interval of $p\text{O}_2 = 1 \times 10^{-11} - 0.21$ atm are presented in Fig. 6. The dependence of SrTiO_3 sample reaches a minimum value corresponding to the equality of hole and electron conductivities ($\sigma_p = \sigma_n$), whereas the dependence of the Co-doped samples is linear. The ambipolar conductivity increases with the increase of Co-content from 0.1 mS cm^{-1} for $x=0$ to 52 mS cm^{-1} for $x=0.25$ at $\log(p\text{O}_2/\text{atm}) = -0.6$.

The study of the oxygen permeability of these materials is important because of their possible use in solid oxide electrochemical devices. Fig. 7 shows the dependence of the oxygen permeability and current of pump on the electromotive force (emf) for $\text{SrTi}_{0.8}\text{Co}_{0.2}\text{O}_{3-\delta}$ at 900°C . Obviously, the sample presents a sufficiently high value of oxygen flow, which is comparable with the value of the oxygen permeability of some of well-known mixed ionic–electronic conductors [16]. The value of the effective ambipolar conductivity calculated from the obtained data of the oxygen permeability for the $\text{SrTi}_{0.8}\text{Co}_{0.2}\text{O}_{3-\delta}$ sample is equal to 30 mS cm^{-1} and is in good agreement with the average ambipolar conductivity obtained from its $\log \sigma \div \log p\text{O}_2$ -dependence that corresponds to 32 mS cm^{-1} .

For a more detailed study of the reduction of cobalt in $\text{SrTi}_{1-x}\text{Co}_x\text{O}_{3-\delta}$, the dependence of the electrical conductivity of the samples on the $p\text{O}_2$ in gas mixtures of $\text{O}_2\text{--H}_2\text{O}$ and $\text{H}_2\text{O--H}_2$ at 900°C was investigated (Fig. 8). Conventionally, the $\log \sigma \div \log p\text{O}_2$ -dependence can be divided into three regions, corresponding to

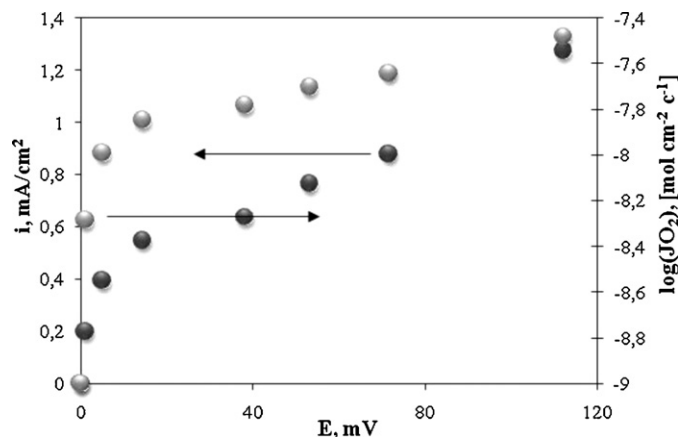


Fig. 7. The dependence of the oxygen permeability and current of pump on the emf for $\text{SrTi}_{0.8}\text{Co}_{0.2}\text{O}_{3-\delta}$ at 900°C .

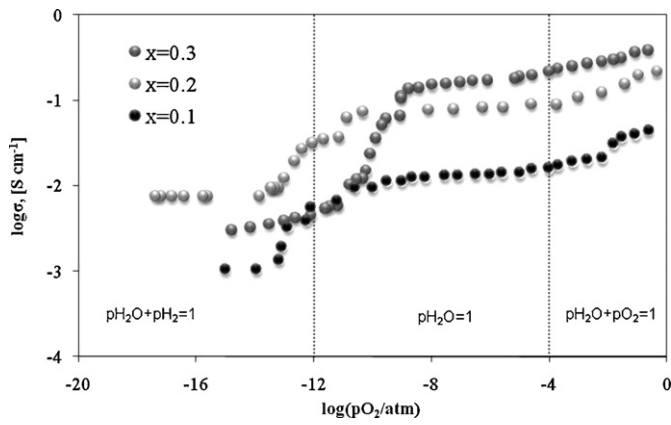
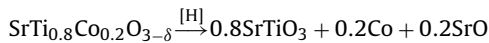


Fig. 8. Oxygen partial pressure dependence of electrical conductivity of $\text{SrTi}_{1-x}\text{Co}_x\text{O}_{3-\delta}$ samples in gas mixture $\text{O}_2\text{--H}_2\text{O}$ and $\text{H}_2\text{--H}_2\text{O}$ at 900°C .

different states of the atmosphere in equilibrium with the sample. The first region corresponds to an atmosphere of moistened oxygen ($x\text{O}_2 + (1-x)\text{H}_2\text{O}$, where $p\text{O}_2 > 1 \times 10^{-5}$, $p\text{H}_2 < 1 \times 10^{-5}$ atm), the second one to the atmosphere of water vapor (oxygen and hydrogen are insignificant ($p\text{O}_2 < 1 \times 10^{-5}$, $p\text{H}_2 < 1 \times 10^{-5}$ atm), and the third one to a mixture of water-hydrogen ($p\text{O}_2 < 1 \times 10^{-5}$, $p\text{H}_2 > 1 \times 10^{-5}$ atm). The graph shows that the decrease in the conductivity of the samples with $x=0.1$, 0.2 and 0.3 , appears to be associated with the reduction of the material occurred at oxygen partial pressures 1×10^{-11} – 1×10^{-10} atm, which correspond to the partial pressure of hydrogen 0.0008 – 0.0023 atm, respectively. The decrease of conductivity occurs at higher value of $p\text{O}_2$ with respect to pumping-out of O_2 from wet oxygen. Fig. 9 shows the XRD patterns of the $\text{SrTi}_{0.8}\text{Co}_{0.2}\text{O}_{3-\delta}$ sample after treatment in humidified H_2 at 900°C for 3 h and following cooling to room temperature in air. The X-ray composition peaks of $\text{SrTi}_{0.8}\text{Co}_{0.2}\text{O}_{3-\delta}$ correspond to the main phase of SrTiO_3 , and the reflections to the phases of CoO , Co_3O_4 and $\text{Sr}_2\text{Co}_2\text{O}_5$. The presence of impurity phases may be due to the destruction of the sample during reduction according to the following equation reaction:



As the cooling occurred in the air, cobalt oxidized back to the oxides CoO and Co_3O_4 , some of which could react with the strontium oxide to obtain the strontium phase, for example, as follows:

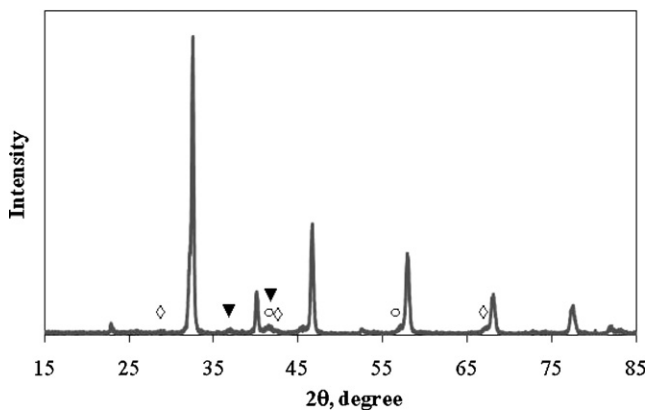
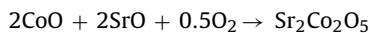


Fig. 9. XRD patterns of $\text{SrTi}_{0.8}\text{Co}_{0.2}\text{O}_{3-\delta}$ sample after treatment in humidified H_2 at 900°C for 3 h and following cooling to room temperature in air. Key: \circ – $\text{Sr}_2\text{Co}_2\text{O}_5$, \blacktriangledown – CoO , \diamond – Co_3O_4 .

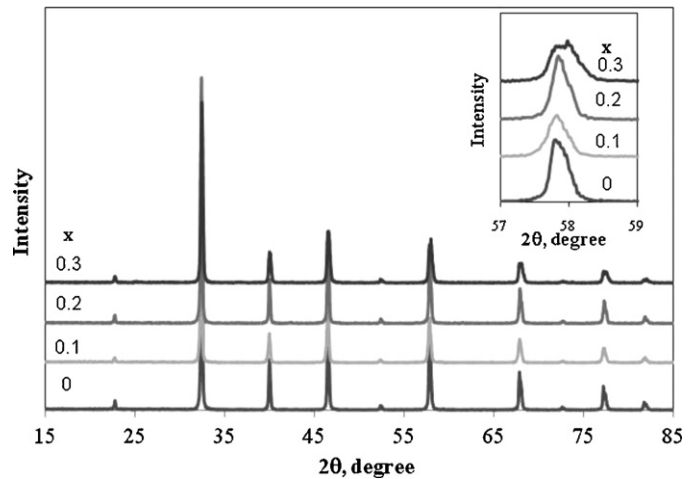


Fig. 10. Room temperature XRD data of $\text{SrTi}_{1-x}\text{Co}_x\text{O}_{3-\delta}$ samples after treatment in pure CO_2 at 750°C for 5 h.

Thus, single-phase materials based on strontium titanate doped with cobalt, are stable only in oxidizing atmospheres ($p\text{O}_2 > 1 \times 10^{-8}$ atm).

It is also of great interest to study the stability of the samples in an atmosphere containing CO_2 , due to the possibility of the formation of strontium carbonate phase. The XRD patterns of the samples after soaking in the atmosphere of CO_2 for 5 h at 750°C are presented in Fig. 10. The samples of SrTiO_3 retain cubic structure, while the structure of the sample $\text{SrTi}_{0.7}\text{Co}_{0.3}\text{O}_{3-\delta}$ changes from cubic to tetragonal (space group $P4/mmm$), which can be observed on the splitting of some characteristic peaks (for example, the response in the interval $57^\circ \leq 2\theta \leq 59^\circ$). Probably, it is related with the presence of the two isostructural phases in the sample with the nominal composition $\text{SrTi}_{0.7}\text{Co}_{0.3}\text{O}_{3-\delta}$. It is known that cobaltites are less stable materials in the atmosphere of CO_2 than the titanates and therefore can react with carbon dioxide with partial destruction of the perovskite structure. The parameters of the elementary cubic cell of the samples with $x=0, 0.1, 0.2$, before and after treatment with CO_2 change slightly, whereas in the case of the sample with $x=0.3$ the lattice parameter increases from 3.895 to 3.899 \AA .

Finally, the linear expansion as a function of temperature for $\text{SrTi}_{1-x}\text{Co}_x\text{O}_{3-\delta}$ samples is presented in Fig. 11. The given dependence can be approximated by a straight line. The values of the thermal expansion coefficient (TEC) were calculated in the temperature interval of 100 – 900°C and the dependence of TEC on the

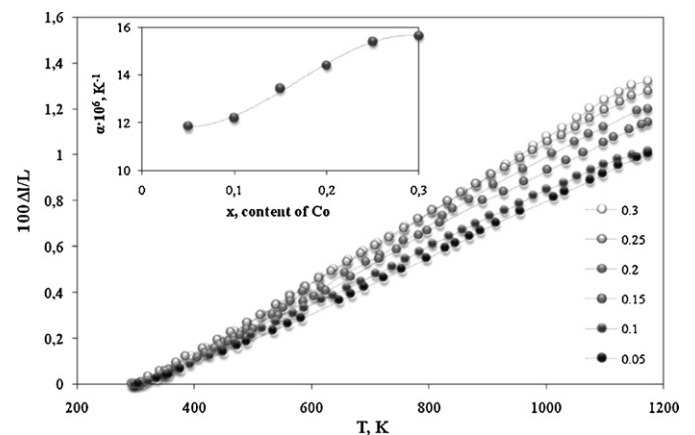


Fig. 11. Thermal expansion data for $\text{SrTi}_{1-x}\text{Co}_x\text{O}_{3-\delta}$ samples. Inset figure: the TEC dependence as a function of Co content.

Co-content is presented (inset Fig. 11). The TEC values of samples increase with the increase of Co-content, from 11.8×10^{-6} ($x=0.05$) to $15.6 \times 10^{-6} \text{ K}^{-1}$ ($x=0.30$). The increase of TEC by the introduction of cobalt is typical for many oxide systems [14].

4. Conclusions

In the present work Co-doped SrTiO₃ solid solutions were prepared by standard ceramic technology at 1150 °C and sintered at 1400 °C. It was found that cobalt doping increases the electrical conductivity and enhances the oxygen permeability of the SrTi_{1-x}Co_xO_{3-δ} membrane. According to the XRD analyses, the samples with $x=0-0.25$ are single-phase (cubic perovskite structure, space group *Pm3m*). In the case of the sample with $x=0.3$ the presence of isostructure phase can be assumed. The unit cell parameters are decreased from 3.906 Å for $x=0$ to 3.894 Å for $x=0.3$. Furthermore, Co-doping results in the increase of total conductivity to 216 mS cm⁻¹ and the increase of ambipolar conductivity to 52 mS cm⁻¹ at $p\text{O}_2=0.21$ atm and 900 °C for $x=0.2$. The maximum value of oxygen permeability of the sample with $x=0.2$ is obtained at 900 °C ($3.3 \times 10^{-8} \text{ mol cm}^{-2} \text{ c}^{-1}$). The Co-doped samples are not stable at low values of $p\text{O}_2$ due to the reduction of Co-ions. On the other hand, the single-phase materials are stable at treatment of CO₂.

Acknowledgments

The present work was supported by the Russian Foundation for Basic Research (grant no. 11-08-00099-a) and The Ministry of Education and Science of the Russian Federation (contract number

16.516.12.6003). The authors would like to thank B.D. Antonov for recording XRD patterns and V.B. Malkov for SEM analysis of the samples. Finally, Prof. P. Tsiakaras is grateful to the Greek Ministry of Development-GSRT “SYNERGASIA” Program (09SYN-32-615: ECHOCO2) for the financial support.

References

- [1] F. Noll, W. Munch, I. Denk, J. Maier, *Solid State Ionics* 86–88 (1996) 711–717.
- [2] A.A. Murashkina, V.I. Maragou, A.K. Demin, E.Yu. Pikalova, P.E. Tsiakaras, *J. Power Sources* 181 (2008) 304–312.
- [3] P. Blennow, A. Hagen, K.K. Hansen, L.R. Wallenberg, M. Mogensen, *Solid State Ionics* 179 (2008) 2047–2058.
- [4] X. Li, H. Zhao, W. Shen, F. Gao, X. Huang, Y. Li, Z. Zhu, *J. Power Sources* 166 (2007) 47–52.
- [5] X. Zhou, O.T. Sorensen, Q. Cao, Y. Xu, *Sens. Actuators B: Chem.* 65 (2000) 52–54.
- [6] X. Li, H. Zhao, F. Gao, N. Chen, N. Xu, *Electrochem. Commun.* 10 (2008) 1567–1570.
- [7] X. Wang, X. Lu, Y. Weng, W. Cai, X. Wu, Y. Liu, F. Huang, J. Zhu, *Solid State Commun.* 150 (2010) 267–270.
- [8] X. Guo, J. Fleig, J. Maier, *Solid State Ionics* 154–155 (2002) 563–569.
- [9] S. Misra, E. Prabhu, K.I. Gnanasekar, V. Jayaraman, P. Chandramohan, M.P. Srinivasan, T. Gnanasekaran, *Mater. Res. Bull.* 44 (2009) 1041–1045.
- [10] V.V. Kharton, L. Shuangbao, A.V. Kovalevsky, A.P. Viskup, E.N. Naumovich, A.A. Tonoyan, *Mater. Chem. Phys.* 53 (1998) 6–12.
- [11] A.A. Murashkina, E.Yu. Pikalova, A.K. Demin, *Russ. J. Electrochem.* 45 (2009) 542–547.
- [12] C. Decorse-Pascanut, J. Berthon, L. Pinsard-Gaudart, N. Dragoe, P. Berthet, *J. Magn. Magn. Mater.* 321 (2009) 3526–3531.
- [13] M.A.F. Souza, R.A. Candeia, S.J.G. Lima, M.R. Cássia-Santos, I.M.G. Santos, E. Longo, A.G. Souza, *J. Therm. Anal. Calorim.* 79 (2005) 407–410.
- [14] V.V. Kharton, L. Shuangbao, A.V. Kovalevsky, *Solid State Ionics* 96 (1997) 141–151.
- [15] C. Pascanut, N. Dragoe, P. Berthet, *J. Magn. Magn. Mater.* 305 (2006) 6–11.
- [16] J. Sunarso, S. Baumann, J.M. Serra, W.A. Meulenber, S. Lui, Y.S. Lin, J.C. Diniz da Costa, *J. Membr. Sci.* 320 (2008) 13–41.